Available online at www.sciencedirect.com
ScienceDirect
Journal of Sound and Vibration 311 (2008) 623–632
JOURNAL OF SOUND AND VIBRATION
www.elsevier.com/locate/jsvi

A new approach to modal analysis of uniform chain systems

William J. O'Connor*, David J. McKeown

UCD School of Electrical, Electronic and Mechanical Engineering, Room 213 Engineering Building, University College Dublin, Belfield, Dublin 4, Ireland

Received 15 December 2006; received in revised form 3 September 2007; accepted 20 September 2007
Available online 25 October 2007

Abstract

A new method is presented to determine the mode shapes and frequencies of uniform systems consisting of chains of masses and springs of arbitrary number with arbitrary boundary conditions. Instead of the classical eigenproblem approach, the system is analysed in terms of circulating waves and associated phase lags. The phasor conditions for the establishment of standing waves determine the vibration modes. The conditions fully specify their shapes and frequencies, and lead to simple, explicit expressions for the components of the modal vectors and the associated natural frequencies. In addition, the form of the phasor diagrams of the modes gives insight into the modal behaviour. The orthogonality of mode shapes also readily emerges. Examples are presented for different boundary conditions. Although not presented, it is possible to extend the approach to non-uniform lumped systems and to forced frequency responses.

1. Introduction and overview

Systems consisting of chains (or strings) of lumped masses and springs are widely used to model flexible structures and devices [1,2]. The classical, mechanical engineering approach to analysing such systems is as follows. Firstly, the equations of motion are established, often in matrix form. These equations are then solved indirectly by first looking for solutions in which the system has synchronous motion. This leads to an eigenproblem in which the eigenvalue emerges as the square of the synchronous frequency, and the eigenvector is the corresponding mode shape. The number of eigenvalue–eigenvector solutions (or natural frequencies and mode shapes) is equal to the number of degrees of freedom. Finally, the general solution to the equations of motion is expressed as a linear combination of the eigensolutions, with coefficients specified by the initial conditions. The orthogonal property of the eigenvectors ensures that this linear combination is unique.

Here a new approach is proposed, based on seeing the motion of the lumped mass–spring system as the superposition of waves travelling in opposite directions within the system, from boundary to boundary. The vibration modes are then seen as standing waves, and the phase conditions for the component standing waves give the mode shapes and the natural frequencies. The phase information required for this approach can be derived in a new way from "wave transfer functions (WTF)", described below and in Refs. [3–5].

*Corresponding author. Tel.: +353 1 7161887; fax: +353 1 2830534.
E-mail address: william.oconnor@ucd.ie (W.J. O'Connor).

0022-460X/$ - see front matter © 2007 Elsevier Ltd. All rights reserved.
doi:10.1016/j.jsv.2007.09.028

The work here is related to classical approaches in the vibrations of long-chain molecules treated as lumped systems, where the phase and frequency relationships of standing waves are determined [6]. That work typically considers the phase of the (already superposed) standing waves, and the modal frequency conditions are established by imposing the boundary conditions on the standing waves. In this paper, by contrast, the phase–frequency relationships are first determined explicitly for each of the component waves, using the WTF model. These component waves are then seen as circulating between reflections at the boundaries, and the phasors describing this motion, when superposed, yield the modal frequencies and shapes.

The system is here assumed to be a uniform series of masses and springs, of arbitrary length, and having any combination of fixed and free boundary conditions at the ends. It is possible to extend the analysis to non-uniform systems, systems with more complex shapes, systems with damping, systems undergoing forced harmonic excitation, and systems with non-geometric boundary conditions, but in this first paper on the topic only uniform, undamped, serial systems will be considered.

2. Wave model of lumped systems

To identify the two-way wave motion, the lumped mass–spring system is represented by a wave model, shown in the lower part of Fig. 1 for a fixed–free system of n masses and n springs. The figure illustrates the case of $n = 3$, but n can take any value. The model has two series of n WTFs, $G(s)$, in opposite directions, the upper branch representing rightwards-going waves, the lower leftwards-going waves. The displacement, $X(i)$ of any mass i, is modelled as the superposition of the corresponding outwards and returning wave components, A_i and B_i:

$$X(i) = A_i + B_i, \quad i = 1, 2, \ldots, n. \tag{1}$$

The wave variables are here taken as displacement from the equilibrium position, with capitals indicating the Laplace domain. The number of transfer functions in each branch equals the number of springs. The ends of the two strings are interconnected by two further blocks, the contents of which depend on the system boundaries. For fixed boundaries this block is (-1), while free boundaries have an interconnecting block of $G(s)$, as illustrated in Fig. 1.

The wave transfer functions (WTFs), $G(s)$, correspond to the transfer function relating the motion between successive masses (or between the ends of any one spring), in the direction of propagation of the motion, in an infinite, uniform, mass–spring system. It is given by Refs. [3–5]:

$$G = G(s) = 1 + \tfrac{1}{2}(s/\omega_n)^2 - \tfrac{1}{2}(s/\omega_n)\sqrt{(s/\omega_n)^2 + 4}, \tag{2}$$

where $\omega_n = \sqrt{(k/m)}$, with m the value of each mass and k the stiffness of each spring.

In the upper branch, motion is propagating to the right, while in the lower it is propagating to the left, so that

$$A_{i+1} = GA_i \tag{3}$$

and

$$B_{i-1} = GB_i. \tag{4}$$

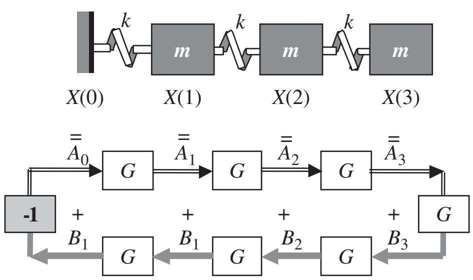

Fig. 1. A wave model of a three mass systems with $X(i) = A_i + B_i$.

The wave model of the system can be validated by confirming that it obeys the system equations of motion and the boundary conditions. The fixed–free case, of arbitrary length, will be taken as an example of wave model validation as follows.

In the s-domain, the equation of motion of any mass, m_i (other than an end mass) is

$$m_i X(i)s^2 = k(X(i-1) - 2X(i) + X(i+1)) \tag{5}$$

or

$$X(i-1) - (2 + (s/\omega_n)^2)X(i) + X(i+1) = 0. \tag{6}$$

Inserting the corresponding model variables (Eq. (1)) gives

$$[A_{i-1} + B_{i-1}] - [2 + (s/\omega_n)^2][A_i + B_i] + [A_{i+1} + B_{i+1}] = 0. \tag{7}$$

From Eqs. (3) and (4) this implies

$$[A_{i-1} + B_{i-1}][1 - (2 + (s/\omega_n)^2)G + G^2] = 0, \tag{8}$$

when G of Eq. (2) is inserted into Eq. (8) the equation of motion is found to be satisfied.

The fixed boundary condition is that

$$A_0 + B_0 = X(0) = 0, \tag{9}$$

which is automatically satisfied because $A_0 = -B_0$.

To check the modelling of the end mass and the free boundary, the transfer function between the last mass and the second last mass is

$$\frac{X(n)}{X(n-1)} = \frac{1}{1 + s^2/\omega_n^2}. \tag{10}$$

In the wave model, such as Fig. 1, this is expressed (by inspection) as

$$\frac{A_n + B_n}{A_{n-1} + B_{n-1}} = \frac{A_{n-1}(G + G^2)}{A_{n-1}(1 + G^3)} = \frac{G}{1 - G + G^2}. \tag{11}$$

Again, on substitution of G, shows that boundary condition equation (10) is indeed satisfied.

Thus the superposed waves (Eq. (1)) in the wave model obey all the equations of motion of the real system, including the boundary equations, and to this extent it models the system exactly.

3. Wave model at constant frequency

The wave model reproduces all the dynamics of the system, including transients, but for modal analysis only steady state, harmonic motion is of interest. The frequency response $G(j\omega)$ of the WTF is shown in Bode diagram form in Fig. 2. The most significant points in the present context is that, at frequencies up to $2\omega_n$, the gain is exactly unity and the phase lag increases monotonically towards $-\pi$ radians (-180°). The phase from $G(j\omega)$ of Eq. (2) is given by

$$\phi = \tan^{-1}\frac{-\omega\sqrt{4\omega_n^2 - \omega^2}}{2\omega_n^2 - \omega^2} \tag{12}$$

with $0 \geqslant \phi \geqslant -\pi$. Rearranging Eq. (12), the frequency, ω, at which a given phase lag, ϕ, occurs, is given by

$$\omega^2 = 2\omega_n^2(1 - \cos\phi), \quad 0 \leqslant \phi \leqslant -\pi. \tag{13}$$

Note that here $\omega_n = \sqrt{(k/m)}$, regardless of the number of masses and springs. When $\omega = 2\omega_n$, successive masses vibrate in anti-phase (with phase difference of $\pm\pi$). This could be considered a cut-off frequency, beyond which wave propagation over significant distances ceases.

Thus, if the system is moving synchronously at a frequency $\omega < 2\omega_n$, the WTF causes a phase lag, ϕ, with unity gain. If the wave variables at this frequency are represented by phasors, the effect of going though each WTF block becomes a simple rotation through ϕ, or multiplication by $e^{j\phi}$, where ϕ is always negative.

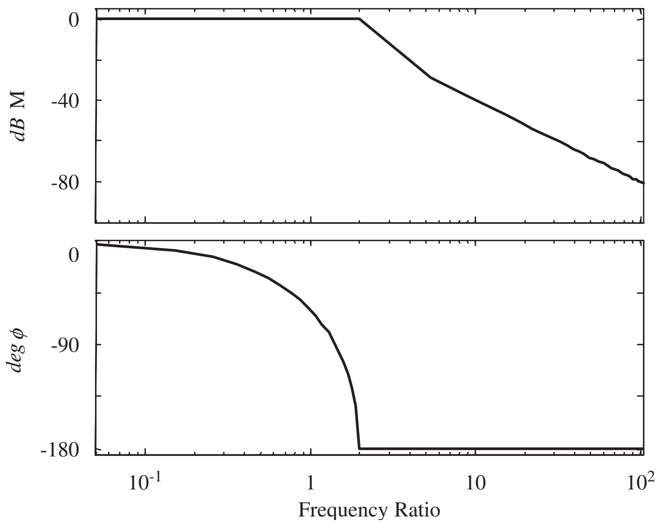

Fig. 2. Bode diagram of $G(j\omega)$.

For the remainder of this paper the variables $X(i)$, A_i, and B_i will be taken as displacement phasors, that is, complex numbers, with magnitude and phase angle (argument), representing displacement variables oscillating at a constant frequency. Phasor A_0 will typically be taken as the reference phasor, having zero phase angle and an arbitrary magnitude which will determine the arbitrary amplitude of the modal vector.

If the system is vibrating in a particular mode, by definition its motion is steady and synchronous. The phasor representation therefore should not vary with time. Thus, in going around the complete loop of the wave model (such as in Fig. 1) and returning to the same point, the total gain should be unity and the total phase an integral multiple of $\pm 2\pi$. From a wave perspective, these two conditions imply the existence of a standing wave at the synchronous frequency. Each way this can happen corresponds to one mode of vibration. The number of possible system modes corresponds to the number of ways the gain and phase conditions can be met and a standing wave established. This perspective is the essence of the method.

The fixed–free case of Fig. 1 will be considered as the main example. This configuration is of wide engineering interest in modelling robots, dynamic structures, cantilevered components, etc. Examples of systems with other boundary conditions will also be considered briefly.

4. Modal analysis of fixed–free system

As has been seen, the fixed–free system with n springs and n masses has $2n+1$ WTFs. At a given frequency below $2\omega_n$, all have unity gain and the same phase lag. The fixed boundary condition block, which multiplies by -1, corresponds to unity gain magnitude and a phase shift of $-\pi$. Thus, the condition that the loop gain be unity is automatically satisfied at frequencies below cut-off. The phase condition is that

$$(2n+1)\phi - \pi = -\alpha 2\pi, \quad 0 \geqslant \phi \geqslant -\pi, \quad \alpha = 1, 2, \ldots, n \tag{14}$$

or

$$(2n+1)\phi = -(2\alpha - 1)\pi \quad \text{with } \alpha = 1, 2, \ldots, n. \tag{15}$$

The number of solutions is found to be equal to the number of springs and masses n, which is the order of the system. Thus, at $n = 1$, $\phi = -\pi/3$ is the only solution with $\phi \geqslant -\pi$. The frequency giving a phase of $-\pi/3$ can be found either from Eq. (13), or graphically from the phase part of the Bode diagram. In either case, the frequency is found to be precisely ω_n. This simply means that for a 1-dof system there is only one mode of vibration and one resonant frequency of $\omega_n = \sqrt{(k/m)}$.

When $n = 2$, there are two solutions to Eq. (15). For a system with n masses, the $\alpha = n$ solutions are

$${}_n\phi_\alpha = -\pi(2\alpha - 1)/(2n+1), \quad \alpha = 1, 2, \ldots, n. \tag{16}$$

Corresponding to these α phase shifts, there will be α modal frequencies and α mode shapes. The mode frequencies are again easily determined from the Bode plot or from Eq. (13). The mode shapes will now be considered.

5. Mode shapes

If A_0 represents a displacement phasor at a particular modal frequency, then the phasor for A_1 will be the same length but rotated through ϕ. Each successive A_i phasor will be related to the previous one by the same rotation. In going around the loop, from A_0 to A_n and then from B_n back to B_0, there will be $2n+1$ such rotations, ending up with a net rotation of $-\pi$. The fixed boundary condition will supply the final rotation of $-\pi$ to get from B_0 back to A_0 again, with a total loop gain of unity and total rotation of -2π as required.

For a 1-dof system, the phasor diagram looks like Fig. 3. The phasors are added tail to head, going around the wave model in sequence from boundary to boundary and back again, with a constant angular change of ϕ at all internal points. This involves successive clockwise rotations, because ϕ is negative (i.e. the phase is lagging). Fig. 4 shows the first mode for a 2-mass, fixed-free system, with common phase change between successive phasors of ${}_2\phi_1 = -\pi/5$. The phasor diagram for the second mode (${}_2\phi_2 = -3\pi/5$) is shown in Fig. 5.

The extension to n masses and springs with n degrees of freedom is obvious. There will then be $\alpha = n$ phasor diagrams, each showing a succession of phasors of equal length rotated successively by a common angle ${}_n\phi_\alpha$.

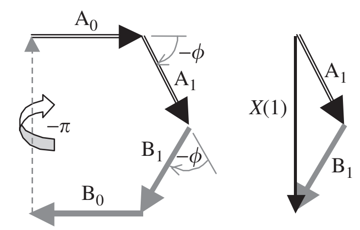

Fig. 3. Phasor diagram for single mass, fixed–free system.

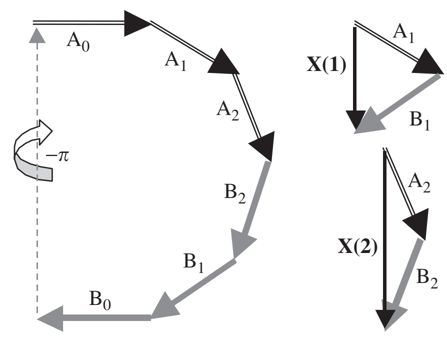

Fig. 4. Phasor diagram for 2-mass, fixed–free system, first mode, ${}_2\phi_1 = -\pi/5$.

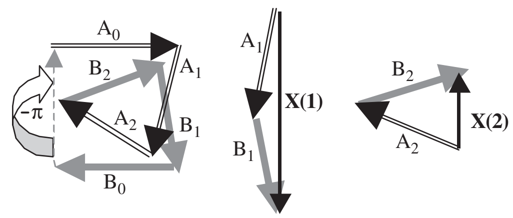

Fig. 5. Phasor diagram for 2-mass, fixed–free system, second mode, ${}_2\phi_2 = -3\pi/5$.

As n (or system size) grows, the phasor diagram of the first mode ($\alpha = 1$) will look more and more like a semicircle, while the nth mode ($\alpha = n$) will look more and more compressed vertically, eventually appearing almost flat.

The displacements, $X(i)$ are obtained (Eq. (1)) by the sum of the two corresponding phasors, A_i and B_i. As can be seen in the diagrams, a pair of phasors A_i and B_i, for a given mass i, are related to each other by a reflection through the horizontal (or A_0 reference direction) and a reversal of direction. The pair add in such a way that the argument of the sum is always $\pm\pi$, with the real parts cancelling.

This leaves the sum of their imaginary parts, which can also be expressed as twice the imaginary part of either. Thus (remembering that here i is an integer index, not $\sqrt{(-1)} = j$)

$$\begin{aligned} X(i)_\alpha &= 2|A_0|\sin(-i\pi(2\alpha-1)/(2n+1)) \\ &= C_\alpha \sin(-i\pi(2\alpha-1)/(2n+1)), \quad i = 1,\ldots,n, \quad \alpha = 1,\ldots,n, \end{aligned} \tag{17}$$

where $C_\alpha = \pm 2\,|A_0|$ is a mode scaling factor, not uniquely defined at this stage. (Modal vectors in general have arbitrary amplitudes, ultimately made definite by initial conditions.)

Although it has taken some reasoning to get there, Eq. (17) is remarkable. It allows the n components of the modal vector, of any mode, α, of the n possible modes in an n-dof system, to be written down almost by inspection, for a uniform system, vibrating under specified boundary conditions (fixed–free in this case). The eigenvalue–eigenvector problem has been avoided and all eigenvector components have been specified explicitly for all modes in a simple, explicit expression.

Furthermore, with the mode shapes established, Rayleigh's Quotient provides a direct way to establish the frequency of each mode:

$$\omega_\alpha^2 = \frac{\sum_2^n (X(i)_\alpha - X(i-1)_\alpha)^2}{\sum_1^n X(i)_\alpha^2}\,\omega_n^2. \tag{18}$$

This third way to get the frequency avoids the need even for a Bode plot of $G(j\omega)$. To get the natural frequency of any mode α, simply insert the appropriate $X(i)_\alpha$ values directly from Eq. (17).

6. Other information in the phasor diagrams

The phasor diagrams provide a new way of seeing well-known results of modal analysis of lumped systems.

The lowest mode provides the simplest phasor diagram, with a single -2π revolution in going from A_0 back to A_0. The total vertical dimension (distance between A_0 and B_0) gives the total vibration amplitude of the system, scaled by A_0. The relative vibration amplitudes of successive masses is seen in the relative values of the phasor sums $X(i) = A_i + B_i$. For the first mode, the displacements become successively larger with distance from the fixed end, and all are in phase.

For higher and higher modes, the phasor diagram becomes more and more convoluted, until at the highest mode it almost reverses direction between each successive phasor. This implies more and more sign changes, or phase inversions, within the modal vector $X(i)$, and, for a given amplitude A_0, the total displacement across the system diminishes. The phasor diagram for the highest frequency mode for systems with larger and larger n becomes more and more compressed vertically, with each phasor approaching a reversal of the previous one as the phase difference approaches $-\pi$. This is approaching the cut-off, at $\omega = 2\omega_n$ and phase lag ϕ of exactly $\pm\pi$.

Velocities and accelerations can be obtained by multiplying the amplitudes by $j\omega$ and $-\omega^2$, respectively. Maximum spring forces are also readily obtained, the force in the ith spring being $k(X(i)-X(i-1))$.

The vector product of two distinct modal vectors, V_α and V_β is

$$\begin{aligned} V_\alpha . V_\beta &= [C_\alpha \sum (A_i + B_i)_\alpha][C_\beta \sum (A_i + B_i)_\beta] \\ &= C_\alpha C_\beta [(A_1 + B_1)_\alpha \sum (A_i + B_i)_\beta + (A_2 + B_2)_\alpha \sum (A_i + B_i)_\beta + \cdots]. \end{aligned} \tag{19}$$

In other words, the vector product involves rotating the entire phasor diagram of one mode (β) by each of the component phasors of the other mode (α), and adding. The net effect is a rotation through -2π and a summation to zero. Thus, the vector product is zero, confirming that distinct modal vectors are indeed mutually orthogonal.

7. Other boundary conditions

To consider other boundary conditions, an example of a fixed–fixed, 3-dof case is shown in Fig. 6, with its corresponding wave model. Corresponding to the 4 active springs, there are 4 WTFs in each branch, upper and lower, giving 8 in total. Because the two boundary conditions can each have a phase shift of $-\pi$, the phase condition becomes $8\phi-\pi-\pi=$ integral multiple of -2π, or, for n masses,

$$(2n+2)\phi - 2\pi = -(\alpha+1)2\pi, \quad \alpha = 1,2,\ldots,n, \quad \phi \geqslant -\pi \tag{20}$$

or

$${}_n\phi_\alpha = -\pi\alpha/(n+1), \quad \alpha = 1,2,\ldots,n. \tag{21}$$

The corresponding modal vectors, $X(i) = A_i + B_i$ are

$$X(i)_\alpha = C_\alpha \sin(-i\pi\alpha/(n+1)), \quad i = 1,\ldots,n, \quad \alpha = 1,\ldots,n \tag{22}$$

with $n=3$ the three possible phases are $-\pi/4$, $-\pi/2$, and $-3\pi/4$ and the phasor diagrams for the three modes are as shown in Fig. 7.

The third possible boundary combination is a free–free system. To take an example of greater engineering interest perhaps, the rotational case of Fig. 8 is considered, rather than a translational example. It has three

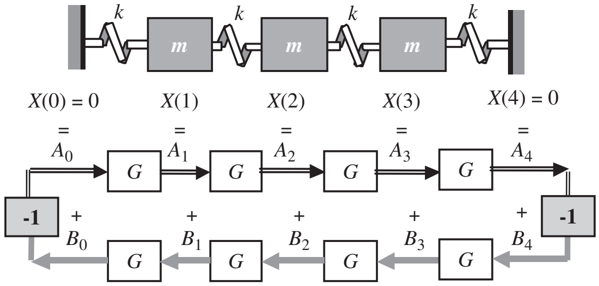

Fig. 6. A fixed–fixed system, with its wave model.

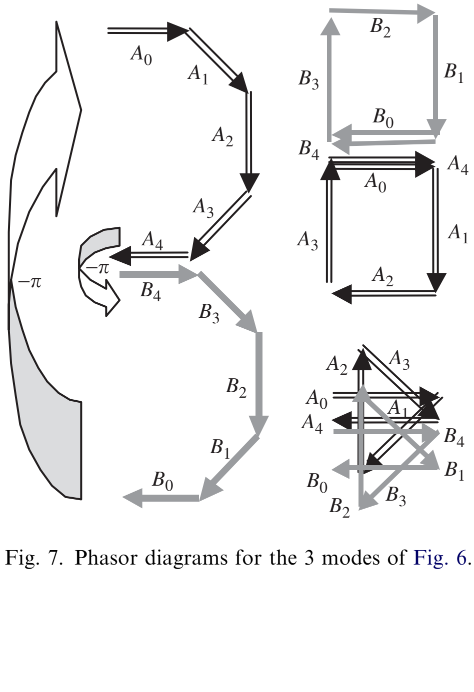

Fig. 7. Phasor diagrams for the 3 modes of Fig. 6.

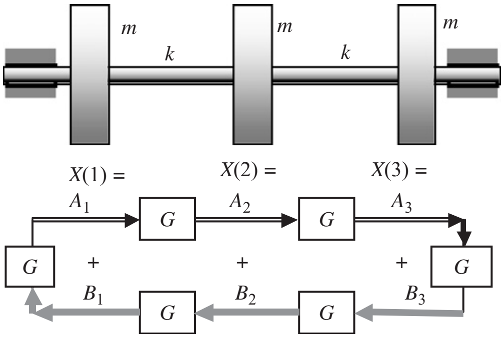

Fig. 8. A free–free system of three masses and two active springs.

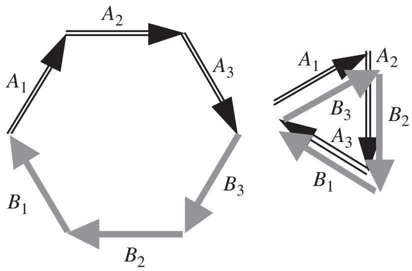

Fig. 9. Phasor diagram of the two vibrational modes of Fig. 8.

rotational inertia elements with moments of inertia m separated by two torsional springs of stiffness k, supported with ideal bearings. (This keeps the notation identical to the translational cases, where X, A_i, and B_i are now angular displacements.) The bearings are the rotational equivalent of free boundaries, with zero torque in the shaft ends.

There are only two active springs in this case, and the corresponding wave model has two WTFs going rightwards (from masses 1 to 2 and 2 to 3) in the upper branch, two in the lower branch, with the each free boundary modelled by another WTF, giving 6 WTFs in total. The absence of any fixed boundary means there is no point in the wave model at which the phase can jump by $-\pi$. This reduces the number of ways the loop phase lag can be a multiple of -2π, with each $\phi \geqslant -\pi$, compared with fixed boundary cases. Specifically, for n inertial elements, or $n-1$ springs,

$$(2(n-1)+2)\phi = 2n\phi = -\alpha 2\pi, \quad \alpha = 1, 2, \ldots, n-1 \tag{23}$$

or

$${}_n\phi_\alpha = -\pi\alpha/n, \quad \alpha = 1, 2, \ldots, n-1. \tag{24}$$

The phasor diagrams again have successive phasors lagging previous ones by ${}_n\phi_\alpha$ of Eq. (24). Unlike in the fixed cases however, there is now no obvious candidate for a reference phasor to set the size and orientation of the phasor diagram. The orientation in Fig. 9 is chosen to achieve the same symmetry as in the fixed cases above, with the real parts of the A_i and B_i phasor pairs again cancelling each other to give purely imaginary terms for the $X(i)$. To achieve this, A_1 has been set to $\frac{1}{2}{}_n\phi_\alpha$ from the vertical, that is, with argument $\frac{1}{2}(\pi + {}_n\phi_\alpha)$, and of arbitrary magnitude. Then

$$\begin{aligned} X(i)_\alpha &= 2|A_1|\sin(\tfrac{1}{2}(\pi - {}_n\phi_\alpha) + {}_n\phi_\alpha i), \quad i = 1, \ldots, n \quad \alpha = 1, \ldots, n-1 \\ &= 2C_\alpha \cos((i - \tfrac{1}{2})\pi\alpha/n), \quad i = 1, \ldots, n, \quad \alpha = 1, \ldots, n-1, \end{aligned} \tag{25}$$

where again C_α is an arbitrary scaling factor for each mode.

For $n = 3$, there are two modes, with ${}_3\phi_1 = -\pi/3$ and ${}_3\phi_2 = -2\pi/3$. Eq. (25) gives the modal vectors, scaled to give whole numbers, as $X_1 = \{1, 0, -1\}$ and $X_2 = \{1, -2, 1\}$. In this simple case, these vector components could be determined almost by inspection of the phasor diagrams of Fig. 9, by adding the phasor pairs directly. The frequencies, by any of the three methods, are ω_n and $\sqrt{3}\omega_n$.

In the free–free case, the number of vibrational modes is one less than the degrees of freedom of the system. The apparently missing mode can be associated with rigid body motion, now possible in the absence of fixed boundaries. While this motion is not vibrational, it can be considered as a modal vector having all equal components, say {1, 1, 1, ...}, and with zero frequency. In the phasor context of this paper, this would have zero phase angle. This "rigid body" or "zero frequency" mode is orthogonal to the vibrational modes properly speaking. To produce zero vector product with {1, 1, 1, ...}, the components of the vibrational modal vectors should individually sum to zero, and have a net phase of $\pm 2\pi$. These properties are indeed observed in the solutions.

8. Discussion, conclusions and further work

A new method to determine the mode shapes and natural frequencies of uniform systems of masses and springs has been presented. Unlike with the traditional eigenproblem approach, the system order has marginal effects on the problem difficulty. Once the concepts have been established, the new method provides a way to obtain mode shapes and frequencies directly and efficiently, with expressions that can be written down almost by inspection, for small or large systems. It also provides new insights into the modal response of a class of vibrating systems.

Phasors are by no means novel in analysing the vibration of lumped mechanical systems. What may be novel rather is the idea of wave-related phasors describing motion propagating in two directions within the system, allowing the overall motion of each part to be resolved into two, counter-propagating component motions, from which the modal results emerge.

The size and orientation of the phasor diagrams is arbitrary. By arbitrarily assigning a magnitude and argument to one phasor, the complete diagram follows. The orientations proposed in the paper simplify the analysis a little, but all results could equally have been obtained, for example, with all X_i horizontal (real), or all at an arbitrary angle with real and imaginary parts. In an undamped system, the sum of phasor-pairs, giving the X_i, will all be parallel, so for any orientation of the diagram their ratios will still be signed real numbers, leading to the same modal vector components derived above.

The phasor diagrams illustrated in the paper are mainly aids to understanding and to developing the equations for the modal vector components. In practice, it would not be necessary to draw them. In any case, they would appear to be more and more entangled (and so less visually informative) for higher modes in higher order systems. The point is that, once the equations have been established in a general form, the phasor diagrams become almost superfluous.

This first paper considers only simply connected, uniform, undamped cases. This means that successive phasors are equal in magnitude and in phase difference. When the masses and springs are not uniform, or when the vibrating system has a more complex morphology, the phase and gain of each wave transfer function are no longer constants for a given mode, and the sums of phasor-pairs will not necessarily be parallel to each other. Nevertheless—at least for string-structured systems—the loop gain and loop phase lag of the corresponding wave model can be expressed as a function of frequency, and so the standing wave conditions can be found quite easily, and the modal features then determined. The analysis therefore is not quite as easy as in the uniform case, but all modal results can still be obtained in a direct way without having to resort to any classical eigensolution methods. The details will be presented in a separate paper. Meanwhile, in addition to introducing the ideas, the present work will provide approximate solutions for systems that are approximately uniform and undamped.

Although not considered above, it is also possible to add a steady harmonic excitation to the model and so determine the forced, frequency response at any frequency, whether close to resonance or not, in a way analogous to that presented in the paper. For example, if the wall in Fig. 1 were vibrating at a given amplitude and frequency, the corresponding phasor, X_0, would constitute an input to the wave model, setting $A_0 = X_0 - B_0$ [4,5]. The model could have a summing junction at the top left-hand corner, with input X_0. This input would also tie down the amplitude of the vibrating system. Again, the magnitude and phase information around the loop would allow the entire system response to be written down, as was done for the modal responses. This extension of the work will be treated in more detail in another paper.

With the easy availability of high power mathematical software and hardware, the computational benefit of the wave approach to modal analysis is arguably of secondary importance. Perhaps the main point of the paper lies in the believed novelty of the approach and in the insights that follow from it.

References

[1] L. Meirovitch, *Dynamics and Control of Structures*, Wiley, New York, 1990.
[2] L. Meirovitch, *Fundamentals of Vibrations*, McGraw-Hill, New York, 2001.
[3] W.J. O'Connor, D. Lang, Position control of flexible robot arms using mechanical waves, *Journal of Dynamics Systems, Measurement and Control—Transactions of the ASME* 120 (3) (1998) 334–339.
[4] W.J. O'Connor, Wave-echo control of lumped flexible systems, *Journal of Sound and Vibration* 298 (4–5) (2006) 1001–1018.
[5] W.J. O'Connor, Wave-based analysis and control of lump-modeled flexible robots, *IEEE Transactions on Robotics* 23 (2) (2007) 342–352.
[6] B. Szigeti, On the torsional vibrations of long chain molecules, *Proceedings of the Physical Society of London Section B* 65 (1) (1952) 19–32.